Numerical simulation of the factors affecting the growth of lithium dendrites

Wenyu Mu[a], Xunliang Liu[a,*], Zhi Wen[a], Lin Liu[b]

[a] School of Energy and Environmental Engineering, University of Science and Technology Beijing, Beijing 100083, China
[b] Department of Mechanical Engineering, The University of Kansas, Lawrence, Kansas 66045, USA

ARTICLE INFO

ABSTRACT

The secondary lithium battery using lithium metal as a negative electrode has attracted more attention due to its extremely high theoretical specific energy. During the charge and discharge cycle, lithium ions are reduced and nonuniformly deposit on the surface of the lithium electrode, which leads to the formation and growth of lithium dendrites. The growth of lithium dendrites can pierce through the separator and causes internal short circuit of the battery as well as battery catastrophes like thermal runaway. The lithium dendrite growth process is complicated and can be affected by various factors. In this paper, a phase field model is developed to simulate the growth process of lithium dendrites, and the effects of anisotropic strength, applied voltage and microstructure of solid electrolyte interphase (SEI) on the growth of lithium dendrites are considered and investigated. The geometric model of solid electrolyte interphase (SEI) is established by numerical reconstruction method. Then, the growth process of lithium dendrites in solid electrolyte interphase (SEI) is investigated, which provides insight on revealing the growth mechanism of lithium dendrites.

1. Introduction

Lithium metal anodes have attracted extensive attention due to extremely high theoretical specific energy (3860 mAh g^{-1}), low density (0.59 g cm^{-3}) and lowest negative reduction potential (-3.040 V vs standard hydrogen electrode). In the 1970 s, Exxon invented lithium batteries with lithium metal as the negative electrode [1–4]. However, due to the safety hazard of lithium dendrite growth, secondary lithium battery using lithium metal as the negative electrode has to be given up. In 1982, the Illinois Institute of Technology found that lithium ions have the property of being embedded in graphite. This process is fast and reversible. The first available lithium ion graphite electrode was successfully produced by Bell Laboratories [1–3]. Until 1991, Sony introduced the first commercial rechargeable lithium-ion battery. Since then, lithium-ion batteries have been widely used, and become one of the commonly used battery types [1–4]. In order to improve the anode performance, a highly conductive metal phase 1T (octahedron) - MoS$_2$ electrode was developed by Wang et al. [5] with a new mechanism of "molybdenum lithium storage". Since MoS$_2$ is a good candidate for anode, Zhang et al. [6] prepared V-Mo-S-Na electrodes using the metal doping method, which present excellent cyclic stability and Li storage rate performance. It is expected to be a high performance anode for lithium ion batteries. In recent years, with the development of electric vehicles and the demand for higher specific energy batteries,

rechargeable lithium batteries using metallic lithium as a negative electrode have once again attracted more and more attention. So far, although many methods have been proposed to suppress lithium dendrites, this problem has not been solved very well.

During the metallic lithium deposition, lithium ions are reduced to lithium on the surface of the lithium electrode and then deposited, which is mainly due to nonuniform lithium ion diffusion in the electrolyte and nonuniform charge distribution on the surface of the lithium electrode [7]. This continuous deposition may result in dendritic structures so called lithium dendrites. The growth of lithium dendrites can pierce through the battery separator as well as causing a short circuit inside the battery and leading to thermal runaway and even explosion. As one of first pioneers, Monroe and Newman [8] simulated electrochemical dendrite growth, and proposed a comprehensive mathematical model for the temporal evolution of dendritic tip height and growth rate in lithium polymer batteries. The growth of lithium dendrites is essentially the evolution process of the lithium electrode-electrolyte interface, and the phase field method can simulate the continuous phase transition at the solid-liquid interface. Guyer et al. [9,10] established a one-dimensional phase field model for studying equilibrium state and electrochemical reaction kinetics, and successfully obtained the spatial distribution of phase field variables, potentials and charges in electrodes and electrolytes under different potential differences. The above model assumes that the electrochemical reaction

kinetics is linear. In order to accurately simulate the complex shape of lithium dendrites during electrodeposition, Liang et al. [10,11] established a one-dimensional nonlinear phase field model to simulate dendrites and related factors. After that, Zhang et al. [12] and Chen et al. [13] proposed a thermodynamically completely self-consistent nonlinear phase field dynamics model. The phase field variables in this model vary nonlinearly with the electrochemical potential. The chemical potential is a function of the electrostatic potential and the concentration of lithium ions. The advantage is that the Butler-Volmer electrochemical reaction kinetic equation can be derived from this model. The model considers the anisotropy of the electrode/electrolyte interface energy and can be applied to any dendritic growth simulation in an unbalanced electrodeposition system [14]. It can be said that the nonlinear phase field model is a powerful tool for investigating the lithium dendrite growth in the batteries.

It is believed that many factors affect the growth of lithium dendrites. These influencing factors not only affect the number of lithium dendrites but also the growth morphology of lithium dendrites. Newman et al. [8] and Akolkar et al. [15] conducted theoretical analysis and draw a conclusion: at higher current densities, the tip of lithium dendrite is smaller; and at lower current density, the tip of lithium dendrite is larger. Through the simulation of lithium dendrites, Zhang et al. [13] and Chen et al. [14] found that lithium dendrite grows faster at larger charging current densities, and the anisotropy strength also affects the growth morphology of lithium dendrites. The more significant influence is that the greater the anisotropy strength, the longer the dendrite is elongated outward. Fukunaka et al. [16] experimentally studied the effect of temperature on the morphology and quantity of lithium dendrites. The lithium dendrites formed under high temperature conditions tend to be "needle-like", and the lithium dendrites under low temperature conditions are closer to "moss". Lithium dendrites formation is less at 10 °C. The increase or decrease in temperature increases the amount of lithium dendrite formed. Through experimental observation, Golozar et al. [17] found that lithium dendrite is not pure lithium and its hardness is higher than pure metallic lithium. Through in situ and ex-situ scanning electron microscopy, two forms of dendrite growth, like moss and hollow needle, was observed in lithium metal batteries. It was found that pressure on batteries can hinder the growth of dendrites. On the surface of the metal lithium electrode, lithium reacts with the electrolyte and a passivation film is formed, which is called as the solid electrolyte interphase (SEI), and plays a vital role in suppressing the growth of lithium dendrites. The concept of passivation film was first proposed by Paled [18] in 1979. It has been shown by existing research that the interface on the surface of the lithium electrode almost completely determines the electrode performance of the lithium metal electrode. It is considered that the SEI of the lithium electrode is composed of two parts. The outer part of the SEI is a porous structure composed of organic matter, and the inside is a dense structure composed of inorganic substances [18–20]. Yurkiv et al. [21] considered the effect of SEI on lithium dendrites by adding stress terms to the phase field equation. Studies have shown that reducing the stress field at the root of lithium dendrites can inhibit the growth of lithium dendrites. Ozhabes et al. [22] calculate and analyze the surface energy of layered materials, multivalent materials, halogen compounds to obtain surface diffusion energy barriers. It has been found that the metal halide has a relatively high surface energy and a low diffusion energy barrier. When it is used as a SEI component, it is expected to obtain a deposition morphology without dendrites. In Chen's article [23], LiF and Li_2CO_3 are thought to be the two main composition of SEI. By the DFT calculation of the surface energy, the conclusion is that it is highly possible that the surface energy anisotropy of Li metal dominates the anisotropy of Li/SEI interface despite the complication in the structure of the multicomponent SEI. However, the influence of the microstructure of SEI on lithium dendrite growth is rarely considered and discussed in the literature. In addition, it is well known the stability of lithium metal batteries highly depends on the SEI above and its
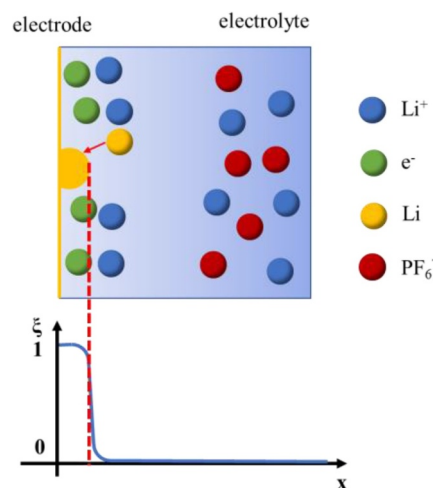

Fig. 1. Schematic diagram of the electrodeposition process distribution of order parameter.

microstructure such as porosity. The different porosity of the SEI is caused by the charge and discharge cycle. Different porosity results in different SEI structures affecting lithium dendrite growth.

In this paper, we focus on the effects of the microstructure of SEI and other factors on lithium dendrite growth. The nonlinear phase field equation was developed to simulate the growth morphology of lithium dendrites. The geometric model of SEI microstructure was established by numerical reconstruction method. Various factors affecting the growth morphology of lithium dendrites such as anisotropy strength, applied voltage and SEI microstructure were explored. The analysis of their effects on the lithium dendrite growth provides new insight on understanding the growth mechanism of lithium dendrites.
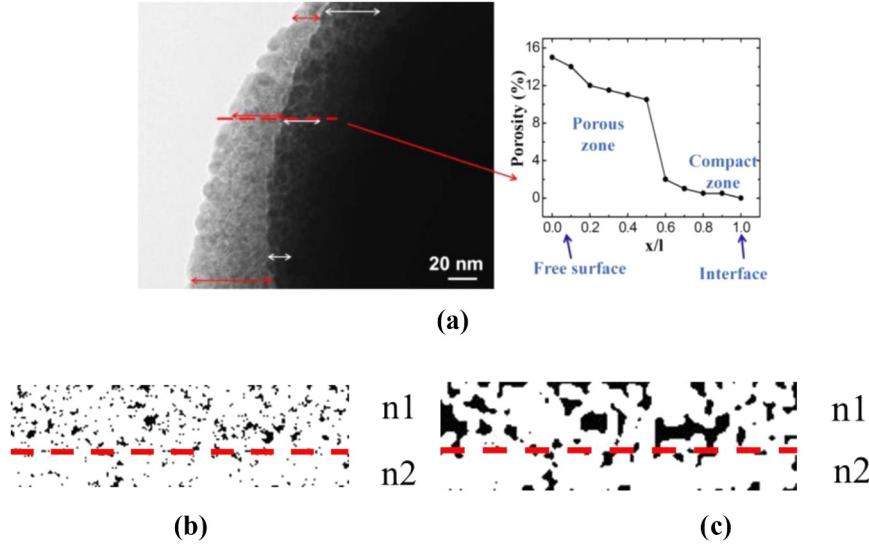
2. Phase field model

2.1. Physical model

This paper assumes that the electrolyte is a dilute solution, and there are enough electrons on the electrode surface for the reaction, as shown in Fig. 1, the left side is the metal electrode, the right side is the electrolyte, and lithium ions react with electrons to form lithium atom. The unevenness of the anode surface causes nonuniform deposition of lithium during the reaction. In some places, the lithium atoms gradually aggregate and grow into lithium dendrites. The protruding portion of dendrites on the surface of the lithium electrode indicates the initial shape of the electrode/electrolyte interface. In phase field simulation, the order parameter ξ is used to indicate the phase morphology of lithium. When ξ is equal to 1, it indicates solid phase lithium in the negative electrode. When ξ is 0, it indicates liquid lithium in the electrolyte. Between 1 and 0 indicates the interface between the two phases. Here the anode is simplified to one surface without considering the structure of the electrode. A tiny semicircle is set on the surface of the electrode as the initial nucleation point for lithium dendrite formation. The order parameter of the semicircle is set to 1, and the rest is 0, indicating the electrolyte. During charging, the lithium ion reacts with the electrons on the surface of the electrode to form lithium atom and deposit, which is described by

$$Li^+ + e^- \leftrightarrow Li \qquad (1)$$

2.2. Phase field equation

The total free energy of the system consists of Helmholtz free energy density, gradient energy density and electrostatic energy density, which can be expressed as

(a)

(b)   **(c)**

Fig. 2. (a) TEM image and porosity analysis of the SEI layer [20] and SEI geometrical model (b) generated by QSGS and (c) after morphological processing (black is pores, white is solid particles).

Table 1
Phase field simulation parameters and their normalized values.

Parameter	Value	Normalized value	Reference
Temperature, T	298 K		
Barrier height, W	3.75×10^5 J m^{-3}	0.25	[13,14,21]
Gradient energy coefficient, κ	5×10^{-5} J m^{-1}	0.01	[13,14]
Interfacial mobility, L_σ	2.5×10^{-6} m^3 J^{-1} s^{-1}	15,000	[14]
Reaction constant, L_η	1.0 s^{-1}	4000	[14]
Diffusion coefficient in electrode, D^e	7.5×10^{-13} m^2 s^{-1}	0.3	[14,21]
Diffusion coefficient in solution, D^s	7.5×10^{-10} m^2 s^{-1}	300	[14,21]
Conductivity in electrode, σ^e	1.0×10^7 S m^{-1}	10^9	[13,14,21]
Conductivity in solution, σ^s	1.0 S m^{-1}	100	[13,14,21]
Symmetric factor, α	0.5	0.5	[13,14,21]
Symmetric factor, β	0.5	0.5	[13,14,21]
Mode of the anisotropy, ω	4	4	[13,14,21]

$$F = \int \left(f_V(\xi, c_i) + \frac{\kappa}{2} |\nabla \xi|^2 + \rho\phi \right) dV \qquad (2)$$

where f_V is the Helmholtz free energy density; κ is the gradient energy coefficient; ρ is the charge density; Φ is the electrostatic potential.

A double-potential function $g(\xi)$ is used to describe the two equilibrium states of the electrode ($\xi = 1$) and the electrolyte ($\xi = 0$) at zero overpotential

$$g(\xi) = W\xi^2(1 - \xi)^2 \qquad (3)$$

where W is the barrier height.

The driving force of the electrode chemical reaction process can be expressed as

$$\Delta G = zF(\phi - \phi^0) = zF\eta \qquad (4)$$

where z is the number of electrons involved in the reaction, taken here as 1; η is the overpotential. When $\eta < 0$, it means that lithium ions in the electrolyte are reduced, and when $\eta > 0$, it means that lithium in the electrode is oxidized.

In order to accurately describe the complex dendrite growth process in the electrodeposition process, a thermodynamically completely self-consistent nonlinear phase field dynamics model is adopted, in which the order parameter changes nonlinearly with the electrochemical potential, and the electrochemical potential is the function of electrostatic potential and lithium ion concentration. The model assumes that the driving force of interface migration is mainly composed of two parts: the reduction of the free energy of the electrode/electrolyte interface

and the electrode reaction. Since the driving force of the electrode reaction related to the overpotential is far greater than the driving force related to the thermodynamic interface energy, the rate of change of the phase interface is linearly related to the decrease of the interface free energy, and is exponentially related to the driving force of the electrode reaction. A simple nonlinear model describing the variation of the order parameter in time and space can be expressed as follows [11–14]

$$\frac{\partial \xi(r, t)}{\partial t} = -L_\sigma \left[\frac{\partial g(\xi)}{\partial \xi} - \nabla \cdot (\kappa \nabla \xi(r, t)) \right]$$
$$- L_\eta h'(\xi) \left[\exp\left(\frac{\alpha \Delta G}{RT}\right) - \tilde{c}_+ \exp\left(-\frac{\beta \Delta G}{RT}\right) \right] \qquad (5)$$

where $\tilde{c}_+$ is the normalized concentration of the lithium ions in the electrolyte; L_σ is the interface mobility; L_η is the reaction-related constant; $h(\xi)$ is an interpolating function, $h(\xi) = \xi^3(6\xi^2 - 15\xi + 10)$, and $h'(\xi)$ is the first derivative of the interpolating function on the order parameter; F is the Faraday constant, 96,485 C mol^{-1}; R is the gas constant, 8.314 J mol^{-1} K^{-1}; T is the temperature; α and β are symmetry factors, the sum of the two is 1, $\alpha + \beta = 1$. The first term on the right side of the equation represents the change caused by the free energy of the electrode/electrolyte interface, and the second term represents the change caused by the electrode reaction.

Anisotropy surface energy is introduced to represent the roughness of the electrode surface. Consider the influence of the free energy anisotropy at the electrode/electrolyte interface [12–14]

(a)

Order Parameter Li⁺ Concentration Electric Potential

(b)
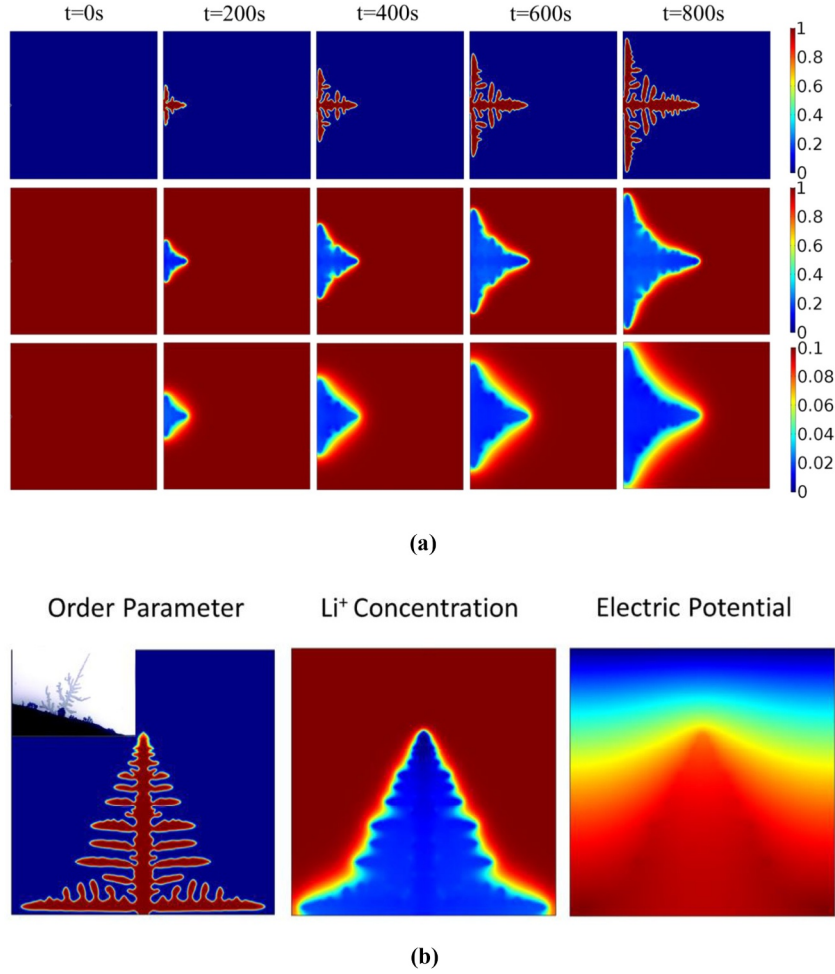
Fig. 3. Lithium dendrite growth process (a) our simulation results (The first row shows the change of the order parameter, the second is the lithium ion concentration distribution, and the third presents the potential distribution.) and (b) simulation results from Ref. [13] (The insert in the corner of the figure of order parameter is experimental observation from Ref. [2]).

$$\kappa = \kappa_0 [1 + \delta \cos(\omega\theta)] \tag{6}$$

where δ is the strength of the anisotropy; ω is the mode of the anisotropy; θ is the angle between the normal vector of the interface and the reference axis.

2.3. Lithium ion diffusion equation

The Nernst-Planck equation is used to describe the diffusion transport of lithium ions. In the electrodeposition process, solid lithium is assumed to be immobile, without diffusion, ignoring the effects of electron transport

$$\frac{\partial \tilde{c}_+}{\partial t} = \nabla \cdot \left[D^{eff} \nabla \tilde{c}_+ + \frac{D^{eff} \tilde{c}_+}{RT} nF \nabla \phi \right] + r_i \tag{7}$$

where D^{eff} is the diffusion coefficient; r_i is the source term.

The source term at the right end of the diffusion equation indicates the consumption of lithium ions during the electrochemical reaction [12–14]

$$r_i = -\frac{c_s}{c_0} \frac{\partial \xi(r, t)}{\partial t} \tag{8}$$

where c_s is the site density of lithium metal; c_0 is the standard bulk concentration of electrolyte solution.

The diffusion coefficient D^{eff} is determined by an interpolation function [12–14]

$$D^{eff} = D^e h(\xi) + D^s(1 - h(\xi)) \tag{9}$$

where D^e is the lithium ion diffusion coefficient in electrode; D^s is the lithium ion diffusion coefficient in electrolyte.

2.4. Charge conservation equation

Assuming the system is electrically neutral, the Poisson equation is used to describe the conservation of current density

$$\nabla [\sigma^{eff} \nabla (\phi(r, t))] = \frac{\partial \rho_t}{\partial t} \tag{10}$$

where σ^{eff} is the conductivity; ρ_t is the space charge density; $\frac{\partial \rho_t}{\partial t}$ is the source term of the conservation of charge equation.
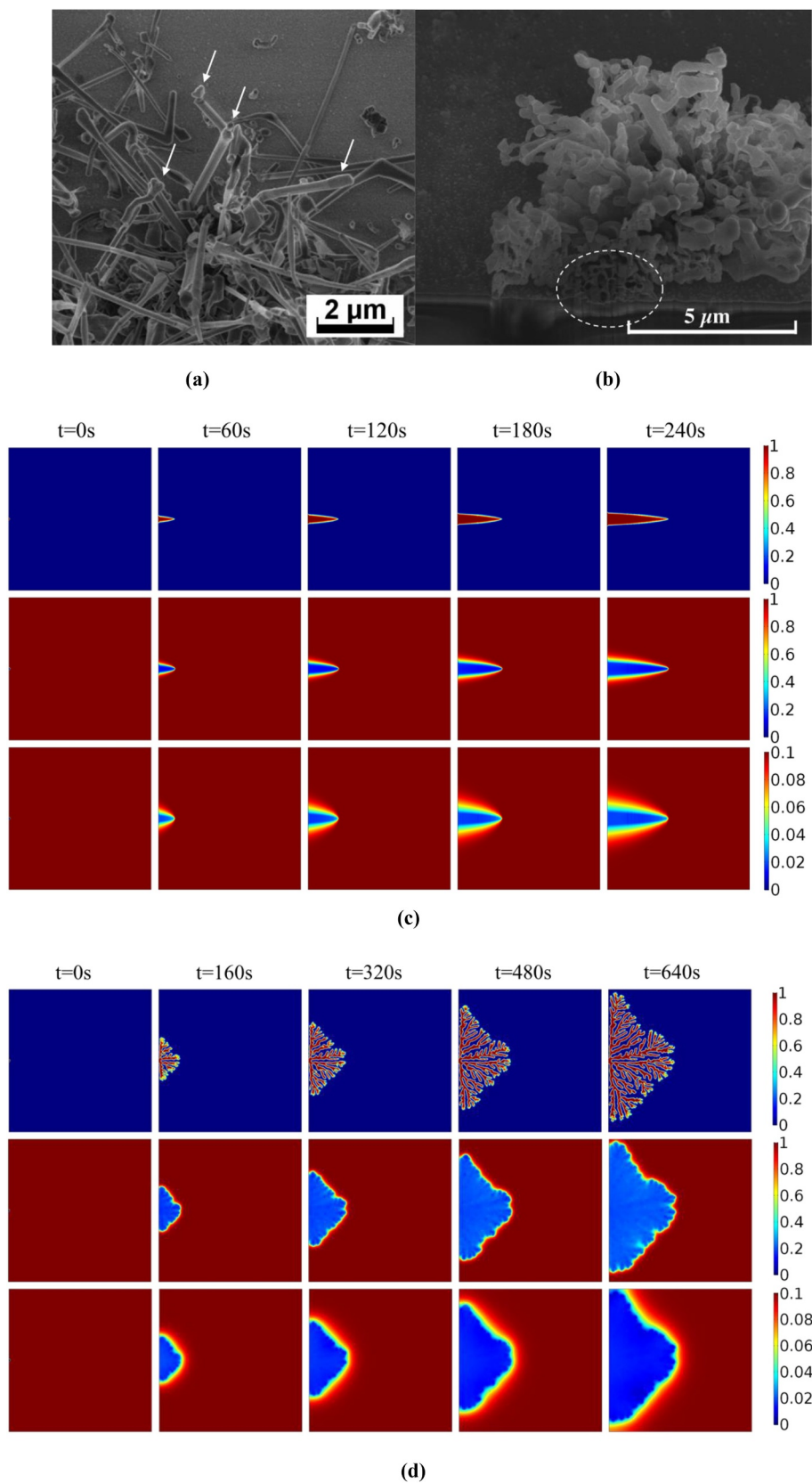
The source term in the equation represents the change in space charge density, that is, the entry or exit of charge during the electrochemical reaction [12–14]

$$\frac{\partial \rho_t}{\partial t} = nFc_s \frac{\partial \xi(r, t)}{\partial t} \tag{11}$$

The conductivity is related to the order parameter and uses the following interpolation form [12–14]

$$\sigma^{eff} = \sigma^e h(\xi) + \sigma^s(1 - h(\xi)) \tag{12}$$

where σ^e is the conductivity of electrode; σ^s is the conductivity of electrolyte.

Fig. 4. SEM image of lithium dendrites (a) needle-like [29] (b) mossy [30] and simulated results of (c) needle-like lithium dendrite growth process and (d) mossy lithium dendrite growth process (The first row shows the change of the order parameter, the second is the lithium ion concentration distribution, and the third presents the potential distribution.).
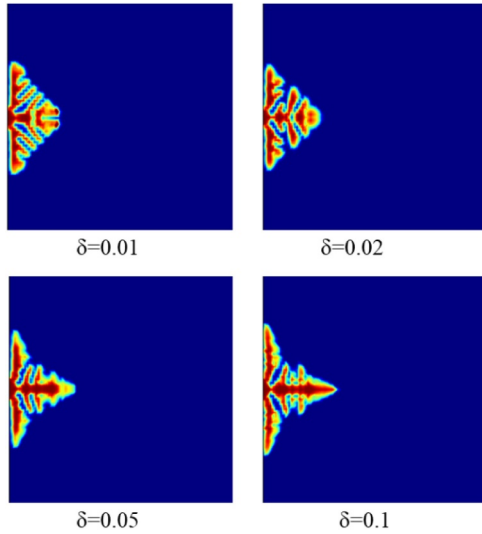
Fig. 5. Variation of lithium dendritic morphology with anisotropy strength.
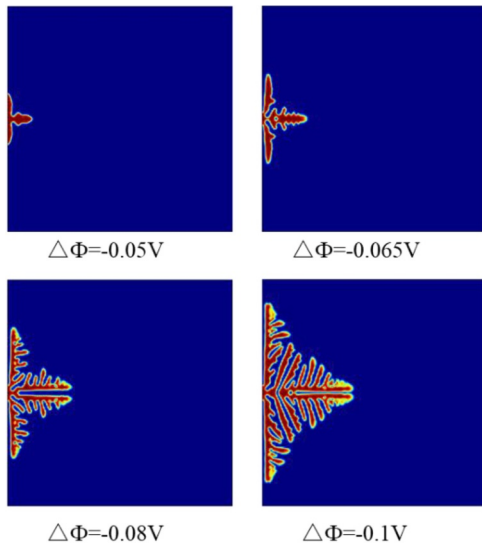

Fig. 6. Lithium dendrite growth morphology at different applied voltages.

2.5. Initial conditions and boundary conditions

In the model, the initial solid-phase lithium is semi-circular, and an initial nucleation point is set in the middle of the left side of the calculation domain. The Dirichlet boundary condition is used. In the concentration field, the electrolyte boundary concentration is set to 1, and the electrode concentration is set to 0. In the electric field, the potential at the electrolyte is higher than the electrode, the potential at the electrode is set to 0, and the potential at the electrolyte is set to 0.1.

2.6. Numerical reconstruction of geometrical model of SEI

For complete understanding of the SEI's effect on lithium dendrite formation the interaction between the different phases and the influence of the stress field should be considered. This significantly complicates the calculations. In this study, only the SEI microstructure is considered to investigate its effect on the lithium dendrite growth for simplicity. The SEI is assumed as porous media composed of inorganic layer and organic layer both with a fixed and different porosity. According to the experimental study on the porosity of SEI by Guan [20], as shown in Fig. 2(a), the porosity of the organic layer is assumed to be 0.15, and the porosity of the inorganic layer is 0.05.

The quartet structure generation set (QSGS) proposed by Wang et al. [24] is used for reconstruction of geometrical model of SEI. This method is widely used for reconstruction of geometrical model of porous media, such as electrode geometry [25], two-dimensional co-continuous ceramic composites finite element model [26], three-dimensional microstructure of coal rock [27], etc. The method controls the formation characteristics of porous structure by four main parameters: solid phase growth nucleation probability P_c; porosity n; growth probability P_d in 8 directions; when there are three phases and three phases or more, considering the interaction between phases and phases, the mutual influence between the two phases is represented by the probability density I_{ij}. The procedure of numerical geometry reconstruction can be described as follows [24]:

(1) The solid phase is randomly arranged in space according to a certain distribution probability P_c.
(2) According to a certain probability, the distributed solid phase grows in the adjacent points in all directions (eight directions).
(3) Repeat (2) until the pore phase reaches a given porosity n.

In the SEI, both the inorganic and organic components are regarded as the solid phase, so there are only two phases, i.e. the solid phase and the pore, regardless of the probability density. The probability of solid-phase growth nucleation is set to 0.1. The growth probability in the direction 1–4 is 0.1, and the growth probability in the direction 5–8 is 0.025. Through a self-developed code running in MATLAB and subsequent morphological processing, the geometrical model of SEI can be reconstructed, as shown in Fig. 2(b) and (c).

2.7. Numerical solution method

The multi-physics coupling calculation software COMSOL Multiphysics 5.3 based on the finite element method is used to solve the phase field equation. In order to speed up the calculation, the normalized number is used for calculation. All the parameters are normalized a characteristic energy density $E_0 = 1.5 \times 10^6\,\mathrm{J\,m^{-3}}$, a characteristic length $l_0 = 100\,\mu\mathrm{m}$, and a characteristic time step $\Delta t_0 = 4000\,\mathrm{s}$ [14]. The parameters are listed in Table 1.

3. Results and discussion

3.1. Lithium dendrite growth morphology

Lithium dendrite growth is related to lithium ion concentration and applied voltage. By solving Eqs. (5), (7) and (10), the growth process is obtained. The simulation results are shown in Fig. 3(a). The lithium dendrite grows in a symmetrical tree-like form. The growth speeds as well as the lengths of the dendrite arms on both sides and in the vertical direction are essentially the same. Along with the tree-shaped lithium dendrites growth, the lithium ion concentration distribution and potential distribution continuously change and display the similar trend. The simulation results are in agreement with the results given by Zhang [13], which are consistent with the experimental results observed by Xu [2], as shown in Fig. 3(b). It can be verified that the phase field model can accurately describe the evolution of the electrode/electrolyte interface and simulate the growth morphology of lithium dendrites.

According to the present research results, the morphology of lithium dendrites can be divided into three types, i.e., dendritic [28], needle-like [29] and mossy [30], the latter two as shown in Fig. 4(a) and (b). For simulating the needle-like lithium dendrites, it can be assumed that the electrodeposition of lithium occurs on the sides of the dendrites and lithium ions are allowed to diffuse only in the y direction [21]. The right direction of orientation is the positive direction of the x-axis, and the upward direction is the positive direction of the y-axis. The simulation results of needle-like lithium dendrite growth are shown in Fig. 4(c). It is found that this type of lithium dendrite grows along the

(a)

(b)
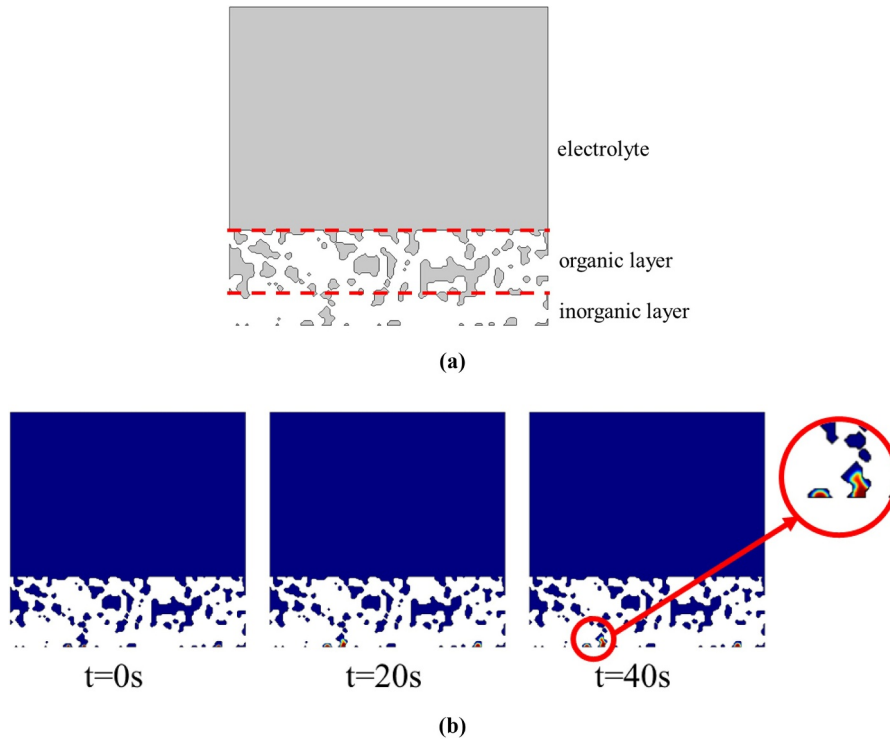
Fig. 7. (a) Reconstructed porous media and models and (b) growth process of lithium dendrites in SEI (a magnified view of the suppressed lithium dendrites in the red circle). (For interpretation of the references to color in this figure legend, the reader is referred to the web version of this article.)

concentration gradient direction, with needle-shaped tip and without branches formed. Compared with the tree-shape dendrite growth, the growth speed of the dendrite tip is more rapid.

For simulating mossy lithium dendrites, it can be achieved by adding a noise term to the free energy function. The noise term is expressed as [21]

$$f_{ns} = h'(\xi)\chi\psi \tag{13}$$

where χ is a random number, and ψ is an amplitude of fluctuation. The simulation results of mossy lithium dendrite growth are shown in Fig. 4(d). It can be seen that the mossy dendrite grows irregularly, with many branches growing out freely and asymmetrically. Apparently, the growth speed of mossy dendrite is more rapid than that of tree-shaped dendrite.

Comparing the simulation results with the experimental observations, they have a good agreement. The needle-shaped dendrites do not have too much bifurcation, while the mossy dendrites have more forks and grow out in all directions. Thus it is assumed that the developed phase filed model is effective in simulating the different growth morphology of lithium dendrites and providing a theoretical basis for exploring its growth effects.

3.2. Effect of anisotropy strength

The strength of interfacial anisotropy indicates the degree of interface surface tension, interface thickness, and interface dynamic anisotropy. From the final shape of dendrite growth, it is reflected in the difference in shape direction after a certain period of growth under specific external conditions; from the crystal growth point of view, it can be regarded as a reference value of the difference in growth rate between the preferential growth direction and other growth directions during dendrite growth. So far, the relationship between anisotropy strength and actual physical parameters is still unclear, but the influence of anisotropy coefficient on dendritic morphology cannot be ignored [31]. The anisotropy strength of the surface energy was changed

to 0.01, 0.02, 0.05 and 0.1, respectively, and the other parameters were kept unchanged. The influence of surface energy anisotropy strength on the growth morphology of lithium dendrites was studied. The simulation results are shown in Fig. 5.

It can be seen from Fig. 5 that as the anisotropy strength δ increases, the growth rate of lithium dendrite increases. When the anisotropy strength is small, the tip of the lithium dendrite is split, and when the anisotropy strength is large, the tip of the lithium dendrite is not split and the tip is sharper and needle-like. At the same time, as the anisotropy strength increases, the growth of secondary dendrite arms slow down and the growth of the primary dendrite arm accelerates. With the increase of anisotropic strength, the dendrite tip becomes sharper and the dendrite grows faster under the same conditions. This is mainly due to the fact that the greater the anisotropic strength, the higher the energy of interfacial anisotropy. Compared with the preferred growth direction, the larger the difference of energy between two directions is, and the more complex the dendrite shape is.

3.3. Effect of applied voltage

The applied voltage $\triangle\Phi$ was changed to $-0.05\,\mathrm{V}$, $-0.065\,\mathrm{V}$, $-0.08\,\mathrm{V}$ and $-0.1\,\mathrm{V}$, respectively, and other parameters were kept unchanged. The effect of applied voltage on the growth morphology of lithium dendrites was studied. The simulation results are shown in Fig. 6.

As seen in Fig. 6, increasing applied voltage leads to a growing acceleration of dendrite formation alongside the occurrence of the splitting phenomenon. As the applied voltage increases, the lithium dendrite tip changes from a complete needle tip structure to a tip-splitting pattern. The applied voltage increases the degree of polarization on the electrode, which in turn affects the diffusion and migration behavior of Li^+ in the electrolyte. Under different polarization conditions, the deposition and accumulation of lithium atoms will be significantly different, which leads to changes in the morphology of lithium dendrites. At the same time, the applied voltage increases and the

(a) Case 1

(b) Case 2

(c) Case 1   **(d) Case 2**
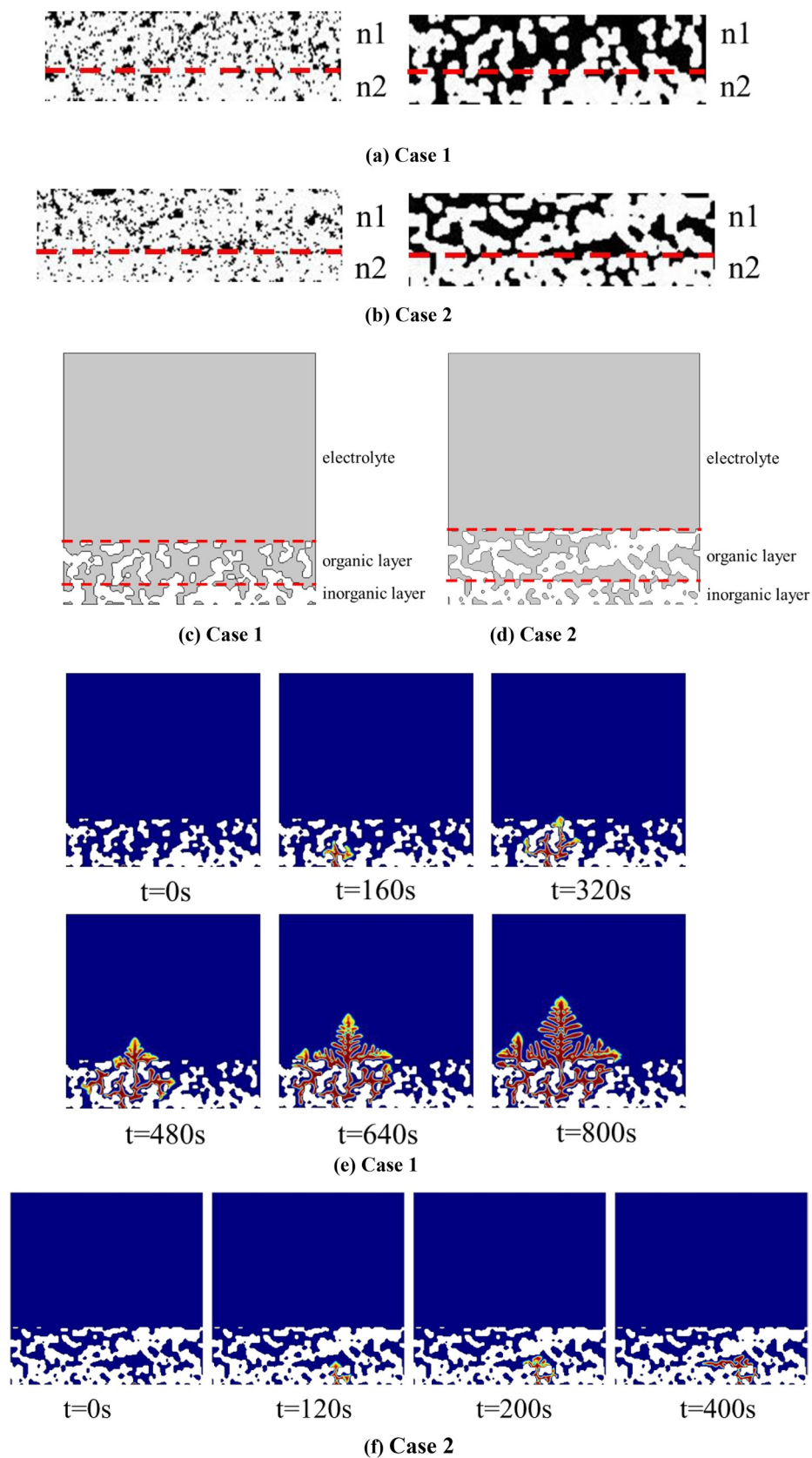
(e) Case 1

(f) Case 2

Fig. 8. SEI geometrical models (a) generated by QSGS and after morphological processing for Case1, (b) generated by QSGS and after morphological processing for Case 2 (black is pores, white is solid particles), reconstructed porous media and models for (c) Case 1 and (d) Case 2, and growth process of lithium dendrite in SEI in (e) Case 1 and (f) Case 2.

current density increases. Monroe and Newman [8] found that the growth rate of lithium dendrites is directly related to the current density. At higher current densities, the growth rate is faster; at lower current densities, the growth rate is slower, and the results obtained by the simulation about the dendrite growth rate agree with it.

3.4. Effect of solid electrolyte interface (SEI)

In order to investigate the effect of SEI, the SEI microstructure was numerically reconstructed using QSGS and the geometrical model including the SEI was established, as shown in Fig. 7(a). Through using COMSOL Multiphysics, the simulation results were obtained, as shown in Fig. 7(b). Due to much low porosity, the SEI structure is dense and the pores are tiny. Since there is a structure in which pores are not connected during the reconstitution process, and during lithium ion transport, lithium ions passing through the SEI are not only transported by the electrolyte, but also migrate through Schottky vacancies in the crystal [18,32]. Therefore, lithium dendrites can still be generated. However, its growth is limited because the SEI cannot be penetrated. Therefore, the lithium dendrite growth is suppressed. It is implied that the lithium dendrites cannot penetrate through the SEI due to its high strength and the pore structure of the SEI suppresses the growth of lithium dendrites. As demonstrated in the magnified area in Fig. 7(b), the lithium dendrites are partially suppressed by the low porosity of the SEI.

However, as a battery is cycled, the destruction and reformation of SEI change its morphology, leading to an increased porosity that is worse at suppressing dendrite formation. Thus, the other two cases were considered for discussion. In the two cases, the porosity of the organic layer n1 is set to 0.2 and the porosity of inorganic layer n2 is set to 0.1, respectively. The difference between them is that there are some connected channels in Case 1 whereas there is no connectivity in Case 2. The reconstructed SEI through QSGS and the established geometrical model are shown in Fig. 8(a)–(d).

The simulation results for the two cases are shown in Fig. 8(e) and (f), respectively. It was assumed that lithium ions were transported by the electrolyte. For Case 1, the lithium dendrites asymmetrically grow along the gap of the porous SEI during the growth process. The side branches grow along the gap into the both sides, and the primary dendrite arm grows up along the gap. After breaking through the porous SEI, lithium dendrite grows in a tree shape with multiple branches. With the growth of side branches, the two parts of dendrites interact with each other and compete for growth. It can be seen that the growth of lithium dendrites is affected by other dendrite arms. The dendrites can only grow along the original gap and be limited in the closed pores. Thus, lithium dendrite growth can be suppressed by control the pore structure of the SEI.

For Case 2, as shown in Fig. 8(f), since the pores are not connected, the lithium dendrites cannot grow outside the SEI. The pore structure and shape of the SEI limit the morphology of lithium dendrite growth, and the morphology of lithium deposit in the pores is asymmetrical and depended on the shape of connected pores. Therefore, it can be deduced that when the pores in the SEI is not through-connected, the dendrites can only grow along the original gap inside the SEI and be limited in the closed pores. Here it is assumed that the lithium dendrites cannot penetrate the SEI, so the growth morphology is significantly affected by the pore connectivity and depends on the SEI microstructure.

4. Conclusions

In this paper, a nonlinear phase field model of lithium dendrite growth is established, and the evolution process of the electrode/electrolyte interface and the three different morphologies of lithium dendrite are simulated. The effects of anisotropic strength and applied voltage on the growth of lithium dendrite are investigated. The morphology of the porous medium layer of the SEI and the growth of

lithium dendrites in the SEI were simulated. The study found that the growth morphology of lithium dendrites is affected by many factors. The growth morphology and velocity of lithium dendrites are related to the surface anisotropy strength and applied voltage. It is believed that the anisotropy strength mainly affects the energy difference between the growth direction of lithium dendrites and the preferred growth direction, resulting in the generation of branches of lithium dendrites. The applied voltage affects the overpotential, and the overpotential as the driving force of the electrochemical reaction affects the growth rate of lithium dendrites, which is consistent with previous research results. For the first time, we used SEI as a porous medium to establish a model by reconstitution method to study the effect of SEI microstructure on the growth of lithium dendrites. In the case where the porous medium layer restricts its growth, the lithium dendrites grow along the gap of the porous medium layer, and when this obstacle is broken, it is still symmetrically grown when not affected by other dendrites. When the porosity is small or the pores are not connected, the growth of lithium dendrites is suppressed and cannot penetrate the SEI. The shape of the SEI limits the growth morphology of the lithium dendrites, and the denser SEI structure can better inhibit the growth of lithium dendrites.

Acknowledgments

References

[1] X. Cheng, R. Zhang, C. Zhao, Q. Zhang, Toward safe lithium metal anode in rechargeable batteries: a review, Chem. Rev. 117 (2017) 10403–10473 http://dx.doi.org/10.1021/acs.chemrev.7b00115.

[2] W. Xu, J. Wang, F. Ding, X. Chen, E. Nasybutin, Y. Zhang, J. Zhang, Lithium metal anodes for rechargeable batteries, Energ. Env. Sci. 7 (2014) 513–537 http://dx.doi.org/10.1039/C3EE40795K.

[3] D. Lin, Y. Liu, Y. Cui, Reviving the lithium metal anode for high-energy batteries, Nat. Nanotechnol 12 (2017) 194–206 http://dx.doi.org/10.1038/nnano.2017.16.

[4] Y. Guo, H. Li, T. Zhai, Reviving lithium-metal anodes for next-generation high-energy batteries, Adv. Mater. 29 (2017) 1700001–1700007 http://dx.doi.org/10.1002/adma.201700007.

[5] L. Wang, Q. Zhang, J. Zhu, X. Duan, Z. Xu, Y. Liu, H. Yang, B. Lu, Nature of extra capacity in MoS2 electrodes: molybdenum atoms accommodate with lithium, Energy Storage Mater. 16 (2019) 37–45 http://dx.doi.org/10.1016/j.ensm.2018.04.025.

[6] Q. Zhang, L. Wang, J. Wang, X. Yu, J. Ge, H. Zhang, B. Lu, Semimetallic vanadium molybdenum sulfide for high-performance battery electrodes, J. Mater. Chem. A 6 (2018) 9411–9419 http://dx.doi.org/10.1039/C8TA00995C.

[7] X. Cheng, Q. Zhang, Dendrite-free lithium metal anodes: stable solid electrolyte interphases for high-efficiency batteries, J. Mater. Chem. A 3 (2015) 727–729 http://dx.doi.org/10.1039/C5TA00689A.

[8] C. Monroe, J. Newman, Dendrite growth in lithium/polymer systems, J. Electrochem. Soc. 150 (2003) A1377–A1384 http://dx.doi.org/10.1149/1.1606686.

[9] J.E. Guyer, W.J. Boettinger, J.A. Warren, G.B. McFadden, Phase field modeling of electrochemistry. I. Equilibrium, Phys. Rev. E 69 (2004) 021603 http://dx.doi.org/10.1103/PhysRevE.69.021603.

[10] J.E. Guyer, W.J. Boettinger, J.A. Warren, G.B. McFadden, Phase field modeling of electrochemistry. II. Kinetics, Phys. Rev. E 69 (2004) 021604 http://dx.doi.org/10.1103/PhysRevE.69.021604.

[11] L. Liang, Y. Qi, F. Xue, S. Bhattacharya, S.J. Harris, L. Chen, Nonlinear phase-field model for electrode-electrolyte interface evolution, Phys. Rev. E 86 (2012) 051609 http://dx.doi.org/10.1103/PhysRevE.86.051609.

[12] L. Liang, L. Chen, Nonlinear phase field model for electrodeposition in electrochemical systems, Appl. Phys. Lett. 105 (2014) 1457–1459 http://dx.doi.org/10.1063/1.4905341.

[13] H.W. Zhang, Z. Liu, L. Liang, L. Chen, Y. Qi, S.J. Harris, P. Lu, L.Q. Chen, Understanding and predicting the lithium dendrite formation in Li-ion batteries: phase field model, ECS Trans. 61 (2014) 1–9 http://dx.doi.org/10.1149/06108.0001ecst.

[14] L. Chen, H.W. Zhang, L.Y. Liang, Z. Liu, Y. Qi, P. Lu, J. Chen, L. Chen, Modulation of dendritic patterns during electrodeposition: a nonlinear phase-field model, J. Power

Sources 300 (2015) 376–385 http://dx.doi.org/10.1016/j.jpowsour.2015.09.055.

[15] R. Akolkar, Mathematical model of the dendritic growth during lithium electro-deposition, J. Power Sources 232 (2013) 23–28 http://dx.doi.org/10.1016/j.jpowsour.2013.01.014.

[16] T. Nishida, K. Nishikawa, M. Rosso, Y. Fukunaka, Optical observation of Li dendrite growth in ionic liquid, Electrochim Acta 100 (2013) 333–341 http://dx.doi.org/10.1016/j.electacta.2012.12.131.

[17] M. Golozar, P. Hovington, A. Paolella, S. Bessette, M. Lagacé, P. Bouchard, H. Demers, R. Gauvin, K. Zaghib, In situ scanning electron microscopy detection of carbide nature of dendrites in Li–polymer batteries, Nano Lett. 18 (2018) 7583–7589 http://dx.doi.org/10.1021/acs.nanolett.8b03148.

[18] E. Peled, The electrochemical behavior of alkali and alkaline earth metals in non-aqueous battery systems—the solid electrolyte interphase model, J. Electrochem Soc. 126 (1979) 2047–2051 http://dx.doi.org/10.1149/1.2128859.

[19] J. Deng, G.J. Wagner, R.P. Muller, Phase field modeling of solid electrolyte interface formation in lithium ion batteries, J. Electrochem Soc. 160 (2013) A487–A496 http://dx.doi.org/10.1149/2.052303jes.

[20] P. Guan, L. Liu, X. Lin, Simulation and experiment on solid electrolyte interphase (SEI) morphology evolution and lithium-ion diffusion, J. Electrochem Soc. 162 (2015) A1798–A1808 http://dx.doi.org/10.1149/2.0521509jes.

[21] V. Yurkiv, T. Foroozan, A. Ramasubramanian, R. Shahbazian-Yassar, F. Mashayek, Phase-field modeling of solid electrolyte interface (SEI) influence on Li dendritic behavior, Electrochim Acta 265 (2018) 609–619 http://dx.doi.org/10.1016/j.electacta.2018.01.212.

[22] Y. Ozhabes, D. Gunceler, T.A. Arias, Stability and surface diffusion at lithium-electrolyte interphases with connections to dendrite suppression, Physics (2015), https://arxiv.org/abs/1504.05799.

[23] L. Chen, Integrating first-principle calculation and phase-field simulation for lithium dendritic growth on the anode of a lithium-ion battery, ASME 2016 Int. Mech. Eng. Congr. Expo. (2016) 9 http://dx.doi.org/10.1115/IMECE2016-65538.

[24] M. Wang, N. Pan, Numerical analyses of effective dielectric constant of multiphase microporous media, J. Appl. Phys. 101 (2007) 227–243 http://dx.doi.org/10.1063/1.2743738.

[25] Z.Y. Jiang, Z.G. Qu, L. Zhou, W.Q. Tao, A microscopic investigation of ion and electron transport in lithium-ion battery porous electrodes using the lattice Boltzmann method, Appl. Energ. 194 (2017) 530–539 http://dx.doi.org/10.1016/j.apenergy.2016.10.125.

[26] Q.X. Wang, H.M. Zhang, H.N. Cai, Q.B. Fan, Modified quartet structure generation set reconstruction of finite element model for co-continuous ceramic composites, Appl. Mech. Mater. 782 (2015) 278–290 http://dx.doi.org/10.4028/www.scientific.net/AMM.782.278.

[27] C. Li, Y. Fang, Y. Ju, Three-dimensional reconstruction of coal's microstructure using randomly packing-sphere and pore-growing and lattice Boltzmann method, J. Nanosci. Nanotechnol. 17 (2017) 6867–6872 http://dx.doi.org/10.1166/jnn.2017.14437.

[28] M.S. Park, S.B. Ma, D.J. Lee, D. Im, S. Doo, O. Yamamoto, A highly reversible lithium metal anode, Sci. Rep-UK 4 (2014) 3815 http://dx.doi.org/10.1038/srep03815.

[29] J. Steiger, D. Kramer, R. Mönig, Mechanisms of dendritic growth investigated by in situ light microscopy during electrodeposition and dissolution of lithium, J. Power Sources 261 (2014) 112–119 http://dx.doi.org/10.1016/j.jpowsour.2014.03.029.

[30] J. Steiger, D. Kramer, R. Mönig, Microscopic observations of the formation, growth and shrinkage of lithium moss during electrodeposition and dissolution, Electrochim Acta 136 (2014) 529–536 http://dx.doi.org/10.1016/j.electacta.2014.05.120.

[31] R. Kobayashi, Modeling and numerical simulations of dendritic crystal growth, Phys. D 63 (1993) 410–423 http://dx.doi.org/10.1016/0167-2789(93)90120-P.

[32] X. Cheng, R. Zhang, C. Zhao, F. Wei, J. Zhang, Q. Zhang, A review of solid electrolyte interphases on lithium metal anode, Adv. Sci. 3 (2016) 1500213 http://dx.doi.org/10.1002/advs.201500213.